JOURNAL OF CATALYSIS 39, 57–72 (1975)

Catalytic Oxidation of Ammonia

I. Reaction Kinetics and Mechanism

N. I. IL'CHENKO AND G. I. GOLODETS

The L. V. Pisarzhevskii Institute of Physical Chemistry of the Academy of Sciences of the Ukrainian SSR, Kiev, USSR

Received August 30, 1973; revised October 17, 1974

The kinetics of ammonia oxidation over oxides of manganese, cobalt, copper, iron and vanadium have been studied. The proposed reaction mechanism involves oxygen adsorption (oxidation of the catalyst surface) and reduction of the surface with ammonia to form the reaction products. The latter step consists of several stages involving the intermediate formation of nitroxyl and imide species. The interaction of imide with nitroxyl leads to nitrogen while the reaction between two nitroxyls results in nitrous oxide. For this model rate equations have been deduced which describe the overall process and the parallel reactions of the formation of N_2 and N_2O. These equations are shown to be in accordance with the experimental data obtained.

It has been found that the selectivity in mild oxidation (N_2 formation) decreases and the selectivity in deep oxidation (N_2O formation) grows with an increase in the surface coverage with oxygen θ. The values of θ increase with the ratio of partial pressures of O_2 to NH_3 (P_{O_2}/P_{NH_3}) in the reaction mixture. The governing role of θ has been supported by experiments in which catalysts were reduced with ammonia in the absence of O_2 in the gas phase.

The reaction mechanism involving the formation of N_2, N_2O and NO is also considered. The corresponding rate equations have been derived, and the expected dependence of specificity on the reaction mixture composition and temperature has been examined.

INTRODUCTION

The oxidation of ammonia over solid catalysts can proceed by way of three main paths:

$$2\ NH_3 + 1.5\ O_2 = N_2 + 3\ H_2O, \quad \text{(I)}$$

$$2\ NH_3 + 2\ O_2 = N_2O + 3\ H_2O, \quad \text{(II)}$$

$$2\ NH_3 \times 2.5\ O_2 = 2\ NO + 3\ H_2O. \quad \text{(III)}$$

With platinum or cobalt oxide catalysts in the temperature range 750–900°C, nitric oxide is a predominant product. Using manganese oxide at lower temperatures (300–400°C) one can obtain nitrous oxide with rather high yield. Over vanadium pentoxide at 500–600°C ammonia is oxidized to nitrogen. In the presence of many catalysts under favorable conditions all three products (N_2, N_2O, NO) are formed in various ratios (*1*,*2*).

Hence, in ammonia oxidation, the problem of *selectivity* of the catalytic action emerges. This distinguishes ammonia oxidation from the majority of the processes of oxidation of inorganic substances (H_2, CO, SO_2, HCl, etc.) for which only catalytic *activity* is essential. At the same time ammonia oxidation appears to be similar to the selective oxidation of various organic molecules. Since the degree of nitrogen oxidation increases in the sequence N_2–N_2O–NO, it is natural to consider N_2 to be a mild oxidation product, while N_2O and NO are products of deep oxidation.

Reactions (I)–(III) are all of practical importance, especially reaction (III) which

is the basis of nitric acid production. The above-mentioned catalysts for ammonia oxidation were discovered empirically; hence it is necessary to search for a theoretical basis of catalyst selection in this reaction.

Most publications on ammonia oxidation refer to platinum catalysts for the NO synthesis operating at high temperatures under a diffusion-controlled regime (*1,2*). Other papers (*3,4*) concern the catalytic properties of oxides. The chemical kinetics of the process have not been much studied and its elementary mechanism is not clear, although numerous hypotheses have been discussed.

In Part I (this paper) of the present work the kinetics of ammonia oxidation have been studied in detail; a reaction mechanism based on kinetic and other experimental data has been proposed, and rational rate equations have been obtained. In Part II (*20*) the relation between the chemical nature of substances and their catalytic behavior is considered. On the basis of the reaction mechanism, the correlation between the activity and selectivity of catalysts and their thermodynamic properties has been established. The results obtained have been used to discuss general regularities in selective catalytic oxidation because essential common features were found in the mechanisms of ammonia oxidation and the selective oxidation of organic substances.

EXPERIMENTAL METHODS

Procedure. The experiments were carried out by a continuous flow method at atmospheric pressure and at low conversions of ammonia (below 20%) so that the reactor can be considered as differential one. With Co_3O_4 additional experiments were made using a nongradient flow-circulation method. The rate values obtained by the both methods proved to be close.

The measurements were carried out at moderate temperatures (below 400°C) when only N_2 and N_2O are formed. In discussing the regularities of the NO formation literature data are used.

The reactor consisted of a 15 mm inside diameter quartz tube, 25 cm long, which was heated externally; catalyst grains were 1–2 mm in size. Along the axis of the reactor was placed a thin well for a thermocouple. The temperature of the catalyst layer was maintained constant within 1°C. Special tests demonstrated the absence of any effect of macrofactors on kinetic data under the conditions of our experiments.

The oxidation was carried out with oxygen; its partial pressure was varied from 0.15 to 0.9 atm by mixing O_2 with helium. Experiments were made under such conditions that water produced in reactions (I) and (II) was not condensed in the apparatus.

The ammonia concentration in the gas stream entering and leaving the reactor was determined by means of titration with standard sulfuric acid. The concentrations of N_2, N_2O and O_2 were determined by gas chromatography using the "Tsvet-4" apparatus with a catharometer; helium was the carrier gas, its pressure was maintained at 2 atm and the flow rate was 60 cm^3/min. For analysis of the gas mixture two columns of CaA 5A molecular sieve were employed; each was 1 m long and 3 mm in diameter. The first column where N_2O was separated from $N_2 + O_2$ operated at 130°C; the second one where nitrogen was separated from oxygen operated at 0°C. Analyzed concentrations were directly proportional to the areas of the peaks. A sampling valve was provided for the withdrawal of aliquots (5 cm^3) of the gas stream for analysis. Before entering the chromatograph a sample passed through traps with anhydrone and solid KOH where ammonia and water were removed. The results of chromatographic analysis as

well as the complete balance in nitrogen indicated that the higher oxides of nitrogen were absent in the products.

Prior to kinetic runs a catalyst was treated with oxygen at 350°C (for MnO_2 at 200°C) over a period of 2 hr. In each case a steady state was attained in the course of catalysis. The values presented below are averages of 4–6 measurements relating to steady state conditions. These values usually agreed within ±5%. The data showed good reproducibility.

A steady state sets in quickly, during only a few minutes. This suggests that phase reduction of the oxides to a new phase did not occur under operating conditions (O_2 excess in the mixture). The color of the catalysts was not altered by the catalytic reaction.

Surface reduction was made in the same apparatus where catalysis was studied. In one series of experiments a catalyst was treated with oxygen for 1 hr, then O_2 was removed from the reactor by the helium stream. After that a NH_3–He mixture was admitted and periodically analyzed at the exit of the reactor. The values of the reaction variables such as temperature, ammonia partial pressure, flow rates (and conditions of the preliminary O_2 treatment) were identical for reduction and catalysis. In these experiments the initial state of an oxide preceding its reduction corresponded to an oxidized surface. In the second series of experiments the catalytic oxidation of NH_3 was carried out prior to reduction; then the reaction mixture was immediately replaced, and the reduction was started. In this case the initial state of the surface was close to its steady state achieved during catalysis.

For calculating rates of formation of N_2 and N_2O (r_{N_2} and r_{N_2O}) the reaction mixture flow velocity was multiplied by the mole fraction of the respective product; the obtained quantities were related to unit surface area and expressed in molecules of the product (N_2 or N_2O) forming per second on 1 cm^2 of a catalyst surface. The rate of the overall process was the sum of rates of the individual reactions, i.e., $r = r_{N_2} + r_{N_2O}$.

Materials. Ammonia (from a cylinder) was purified by passing through a column with solid KOH; the system of the purification of O_2 (from a cylinder) involved columns with KOH and $CaCl_2$. Helium (of "high purity" grade) was dried by passing through a column with molecular sieves. Oxygen contained small amounts of N_2

TABLE 1
CHARACTERISTICS OF THE CATALYSTS

Catalyst	Method of preparation	Specific surface area (m^2)	Sample wt (g)	Temp range for NH_3 oxidation (°C)	Initial temp of N_2O decomposition (°C)
Co_3O_4	Decomposition of cobalt nitrate at 400°C	5.25	11.25	130–170	280
MnO_2	Commercial reagent	24.6	3.63	120–155	410[a]
CuO	Decomposition (500°C) of cupric hydroxide obtained by interaction of $Cu(NO_3)_2$ with NH_4OH	0.92	10.79	220–260	400
Fe_2O_3	Decomposition (500°C, in air stream) of ferric hydroxide obtained by interaction of $Fe(NO_3)_3$ with NH_4OH	22.1	6.72	220–270	500
V_2O_5	Commercial reagent	4.5	8.81	260–320	

[a] After (7).

which were analyzed and taken into account in calculating rates of the formation of N_2 resulting from ammonia. Table 1 gives information about the catalysts studied. Specific surface areas were determined chromatographically by means of N_2 thermal desorption.

RESULTS AND DISCUSSION

Ammonia Oxidation in the Absence of Catalysts

The oxidation of ammonia in the absence of a catalyst started at 380–400°C. With the NH_3–O_2 reaction mixture in which ammonia partial pressure was 0.1 atm, ammonia conversion at 400°C and a 50 cm^3/min flow rate was 4.4%. The reaction products were N_2 and H_2O only. According to Stephens and Pease (*5*) homogeneous noncatalytic oxidation of ammonia proceeds as a chain radical process.

The catalytic oxidation took place at temperatures below 380°C (see Table 1) and in most cases nitrous oxide was formed in addition to nitrogen. A striking similarity has been found between the catalytic oxidation of ammonia over oxides and the essentially heterogeneous process of the reduction of the oxides by ammonia (see below). It proves that ammonia oxidation is entirely a heterogeneous reaction under the conditions studied.

Dependence of Rates on Contact Times and Reaction Mixture Composition

One can assume the following general ways of forming the reaction products.

1. Both nitrogen and nitrous oxide are entirely originated from ammonia and oxygen (independent paths):

$$NH_3 + O_2 \begin{cases} \xrightarrow{\text{Cat}} N_2 \\ \xrightarrow{\text{Cat}} N_2O \end{cases} \qquad \text{(A)}$$

2. Nitrous oxide is formed from ammonia and oxygen while nitrogen is produced either by the subsequent decomposition of N_2O or by the reduction of N_2O with ammonia (consecutive schemes):

$$NH_3 + O_2 \xrightarrow{\text{Cat}} N_2O \xrightarrow{\text{Cat}} N_2 + O_2, \qquad \text{(B.1)}$$

$$NH_3 + O_2 \xrightarrow{\text{Cat}} N_2O \xrightarrow[NH_3]{\text{Cat}} N_2. \qquad \text{(B.2)}$$

The oxidation of N_2 to N_2O is impossible thermodynamically.

If scheme (B.1) or (B.2) is true the observed rate of N_2O formation should decrease while the rate of N_2 formation should increase with increasing contact time τ. If scheme (A) is true, the above rates as well as the selectivity should not depend on τ. Figure 1 demonstrates the relation between contact times and rates r_i of the formation of N_2 and N_2O for the catalysts MnO_2 and Co_3O_4. Among metal oxides these catalysts exhibit the highest activity and selectivity in N_2O. In these experiments the partial pressures of the initial reactants were practically constant whereas the partial pressures of the products varied by several times. The observed independence of S_{N_2O} and r_i on τ shows reactions (I) and (II) to proceed according to scheme (A) (i.e., by parallel ways) under

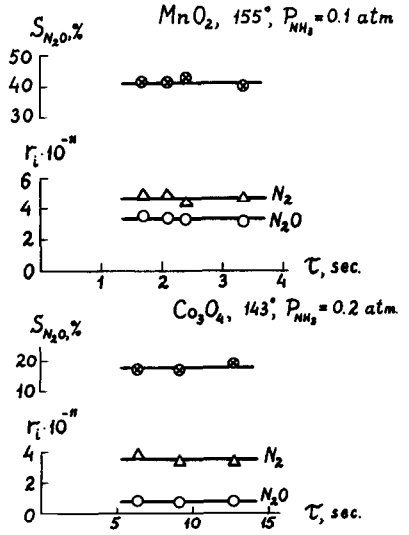

FIG. 1. Rates of the formation of N_2 (△) and N_2O (○) [r_i (molecules/cm^2·sec)] and selectivities in N_2O (⊗) versus contact time τ.

the investigated conditions (at small concentrations of products).

N_2O decomposition over oxide catalysts occurs at substantially higher temperatures than ammonia oxidation. This is additional evidence against scheme (B.1). Table 1 presents the initial temperatures of the N_2O catalytic decomposition (6). Total surface areas of samples used by Saito *et al.* (6) were 3–5 times lower than those in our experiments, but the N_2O partial pressure was two orders higher than the utmost possible value of P_{N_2O} in ammonia oxidation. Because N_2O decomposition follows first order kinetics (6) initial temperatures of N_2O decomposition during ammonia oxidation should be still much higher.

The observed independence of the rates on τ also suggests that there is no retardation of the process by its products.

Figures 2 and 3 demonstrate the dependence of the overall process rates and rates of reactions (I) and (II) upon partial pressures of ammonia and oxygen for different catalysts. Similar patterns have been obtained at other temperatures.

Reaction Mechanism and Rate Equations

We have failed in the attempts to treat our kinetic data using a Langmuir-type approach. The power rate law treatment involving variable kinetic orders appeared to be formal since we would obtain only empirical relations that provide poor infor-

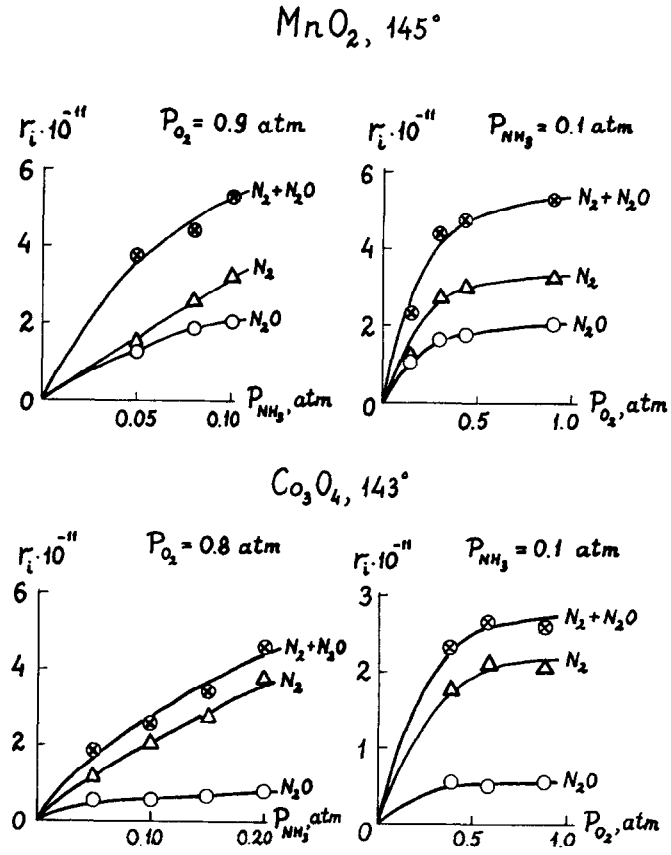

FIG. 2. Dependence of rates of the overall process and the formation of N_2 and N_2O upon P_{NH_3} and P_{O_2}. Catalysts: MnO_2, Co_3O_4.

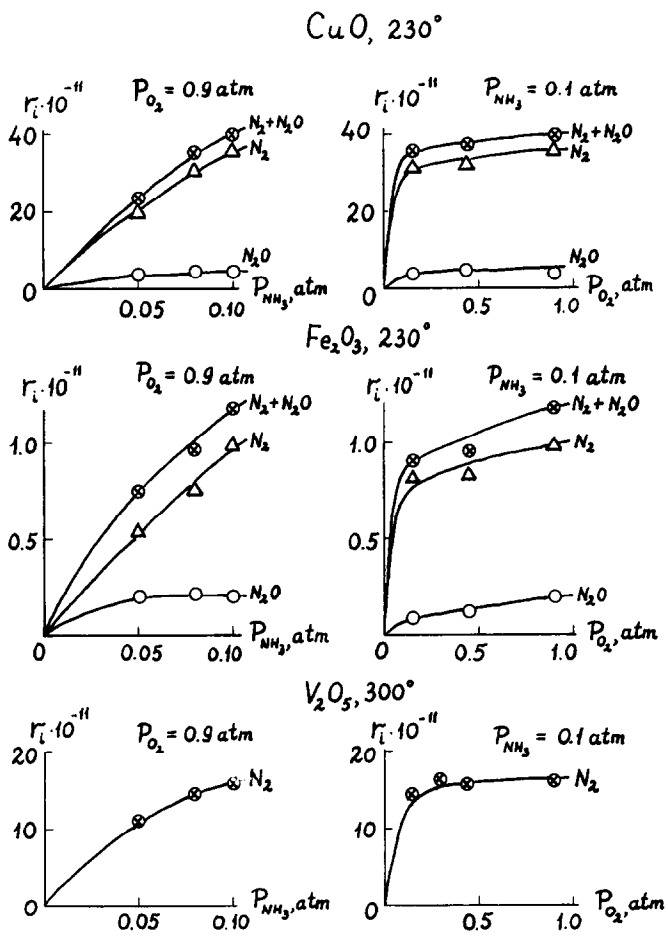

FIG. 3. Dependence of rates of the overall process and the formation of N_2 and N_2O upon P_{NH_3} and P_{O_2}. Catalysts: CuO, Fe_2O_3, V_2O_5.

mation about mechanism. The following reaction mechanism (19) has proved to be acceptable for the interpretation of all the experimental data obtained (here and below symbols in parentheses denote surface species, and empty parentheses mean vacant surface sites):

	Stoichiometric nos.[a]	
	$N^{(I)}$	$N^{(II)}$
1. $O_2 + (\ ) \rightarrow (O_2) \xrightarrow{(\ )}_{\text{fast}} 2(O)$	1.5	2
2. $NH_3 + (O) \rightarrow (NH) + H_2O$	2	2
3. $(NH) + (O) \rightleftarrows (HNO)$	1	2
4. $(NH) + (HNO) \rightarrow N_2 + H_2O + 3(\ )$	1	0
5. $(HNO) + (HNO) \rightarrow N_2O + H_2O + 4(\ )$	0	1

(IV)

[a] $N^{(I)}$: $2NH_3 + 1.5O_2 = N_2 + 3H_2O$; $N^{(II)}$: $2NH_3 + 2O_2 = N_2O + 3H_2O$.

In the first stage oxygen adsorption takes place resulting in the transient formation of molecular anion-radicals of oxygen which, according to ESR data (*8*), are readily converted into atomic anions. In the second stage, ammonia comes into contact with the surface covered by adsorbed oxygen and forms imide-type species (NH) which are further transformed into nitroxyl (HNO) in the course of the third (quasi-equilibrium) stage. The participation of these species in the reaction has already been postulated (*1*). Nitrogen is produced in the fourth stage as a result of the interaction of (NH) and (HNO), while nitrous oxide results from recombination of two nitroxyls.

All the stages except the third one are supposed to be irreversible. According to (IV), each (O) and each (NH) species occupies one elementary surface site while (HNO) requires two sites. The latter assumption will be specially proved later.

Ammonia oxidation is a complex reaction proceeding by several routes. In the case under consideration, when the only nitrogen-containing products are N_2 and N_2O, the number of linearly independent (basic) routes after the Horiuti rule (*9*) is equal to 2. The sets $N^{(I)}$ and $N^{(II)}$ of stoichiometric numbers of stages presented on the right side of scheme (IV) correspond to the routes which are chosen here as basic ones. The overall Eqs. (I) and (II) refer to the first and the second route, respectively.

Assuming the reaction to occur in the ideal adsorbed layer, the surface coverage with atomic oxygen θ being much higher than that with other species, one can write the following rate equations for irreversible stages:

$$\begin{aligned} r_1 &= k_1 P_{O_2}(1-\theta), \\ r_2 &= k_2 P_{NH_3}\theta, \\ r_4 &= k_4 \theta_I \theta_{II}, \\ r_5 &= k_5 \theta_{II}^2. \end{aligned} \tag{1}$$

Here r_1, r_2, r_4, r_5 are rates of the stages, and k_1, k_2, k_4, k_5 are rate constants; θ_I and θ_{II} denote surface coverages with (NH) and (NHO) species, respectively. The third stage equilibrium constant is

$$K_3 = \frac{\theta_{II}}{\theta_I \theta}. \tag{2}$$

For deducing rate equations let us use the conditions of steady state of stages (*10*): $\nu_s^{(I)} r^{(I)} + \nu_s^{(II)} r^{(II)} = r_s - r_{-s}$, where $\nu^{(I)}$ and $\nu_s^{(II)}$ are the stoichiometric numbers of stage s for the basic routes $N_s^{(I)}$ and $N_s^{(II)}$; $r_s^{(I)}$ and $r^{(II)}$ are rates for these routes; r_s and r_{-s} are rates of stage s in the forward and backward directions (for irreversible stages the difference $r_s - r_{-s}$ is practically equal to r_s). Taking Eqs. (1) and (2) into account we arrive at the following equations for rate of the overall process, r, and for rates of the formation of nitrogen and nitrous oxide:

$$r = \tfrac{1}{2} k_2 P_{NH_3}\theta = \frac{\tfrac{1}{2} k_1 k_2 P_{O_2} P_{NH_3}}{k_1 P_{O_2} + \nu k_2 P_{NH_3}}, \tag{3}$$

$$r_{N_2} = r^{(I)} = \frac{\mu}{\mu + \theta} \cdot r, \tag{4}$$

$$r_{N_2O} = r^{(II)} = \frac{\theta}{\mu + \theta} \cdot r, \tag{5}$$

where

$$\mu = \frac{k_4}{k_5 K_3}, \tag{6}$$

and the surface coverage with atomic oxygen will be

$$\theta = \frac{k_1 P_{O_2}}{k_1 P_{O_2} + \nu k_2 P_{NH_3}} = \frac{(k_1/k_2) \cdot (P_{O_2}/P_{NH_3})}{(k_1/k_2) \cdot (P_{O_2}/P_{NH_3}) + \nu}. \tag{7}$$

The stoichiometric coefficient ν indicates how many O_2 molecules are expended for the oxidation of one molecule of ammonia; this quantity is equal to $\nu_{N_2} S_{N_2} + \nu_{N_2O} S_{N_2O}$ where ν_{N_2} and ν_{N_2O} are the ratios of the stoichiometric coefficients of O_2 to NH_3 in Eqs. (I) and (II), and S_{N_2} and S_{N_2O} are the

selectivities in N_2 and N_2O. The value of ν depends upon the reaction conditions which determine S_{N_2} and S_{N_2O}, but in our experiments for each catalyst ν varied slightly. For example, an average value of this coefficient, $\bar{\nu}$, for MnO_2 was 0.86 ± 0.02 and for CuO $\bar{\nu} = 0.79 \pm 0.01$.

Comparison of Rate Equation for Overall Process with Experimental Data

If the overall process rate equation (*3*) is valid, one must obtain a straight line relationship on the plot of P_{O_2}/r against P_{O_2}/P_{NH_3} because

$$\frac{P_{O_2}}{r} = \frac{2\bar{\nu}}{k_1} + \frac{2}{k_2} \cdot \frac{P_{O_2}}{P_{NH_3}}. \qquad (8)$$

Figure 4 shows this relationship to be really observed for MnO_2 and CuO at various temperatures. The same relations

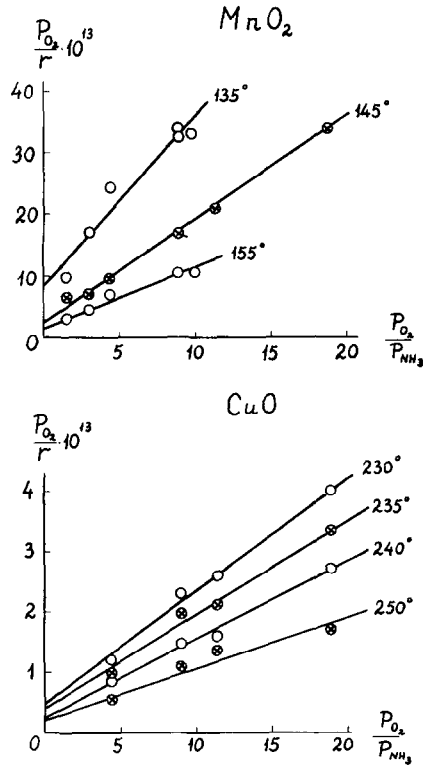

FIG. 4. (P_{O_2}/r)–(P_{O_2}/P_{NH_3}) plots for MnO_2 and CuO.

TABLE 2

RATE CONSTANTS [k_1 AND k_2 (molecules/cm²·sec·atm)] FOR FIRST TWO STAGES OF SCHEME IV

Catalyst	t (°C)	$k_1 \times 10^{-13}$	$k_2 \times 10^{-13}$
MnO_2	135	0.20	0.73
	145	0.66	1.21
	155	1.12	2.00
Co_3O_4	143	0.26	0.61
CuO	230	3.43	10.58
	235	3.98	12.74
	240	5.13	16.13
	250	6.86	23.80
Fe_2O_3	230	0.21	0.26
	250	0.38	0.55
	255	0.35	0.66
	265	0.49	0.84
V_2O_5	260	1.67	1.11
	290	6.50	2.57
	300	7.13	3.58
	310	10.70	4.25

are observed for other catalysts. The slope is $2/k_2$ and the intercept on the ordinate is $2\bar{\nu}/k_1$; using these quantities, rate constants for the first two stages can be found. The corresponding data given in Table 2 have been calculated by means of the least squares method.

The temperature dependence of k_1 and k_2 obeys the Arrhenius equation (Fig. 5) which also proves the validity of Eq. (3). The obtained activation energies for oxygen adsorption (E_1) and those for the interaction of ammonia with adsorbed oxygen (E_2) are presented in Table 3.

Table 3 also shows the standard activation entropies ΔS_2^* for the second stage. These quantities were calculated employing the well-known absolute rate theory equation adapted for surface processes (*11*). The experimental values of E_2 and k_2 were used; the latter were expressed in molecules/gL·sec·atm where gL is the product of the number of possible positions of the activated complex (when

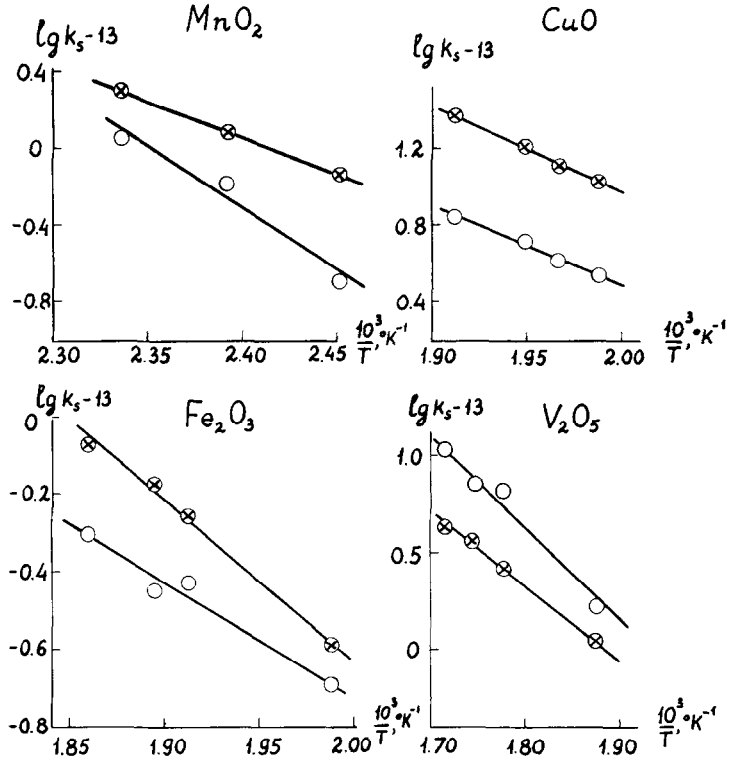

FIG. 5. The Arrhenius plots for rate constants of the first (○) and the second (⊗) stages.

one of the sites occupied by it is fixed) and the number of elementary sites per 1 cm^2; $gL \approx 10^{15}$ cm^{-2} (*11*). The transmission coefficient was taken as usual to be unity. The ΔS_2^* values obtained are approximately constant for all the catalysts studied ($\Delta S_2^* = -30 \pm 3$ e.u.); this suggests that the composition and structure of the activated complexes formed on the different catalysts are similar.

TABLE 3
ACTIVATION ENERGIES FOR FIRST TWO STAGES AND ENTROPY OF ACTIVATION FOR THE SECOND STAGE

Catalyst	E_1 (kcal/mole)	E_2 (kcal/mole)	ΔS_2^* (e.u.)
MnO_2	30	17	−29
CuO	20	20	−27
Fe_2O_3	16	21	−31
V_2O_5	23	20	−33

According to (*12*) the ΔS_2^* values are associated with equilibrium of the formation of the second stage activated complex from gaseous ammonia and adsorbed oxygen, i.e., $\Delta S_2^* = S^* - S^0_{NH_3} - S^0_{(O)}$ where S^* is the standard entropy of the activated complex, $S^0_{NH_3}$ the standard entropy of gaseous ammonia, and $S^0_{(O)}$ the standard entropy of adsorbed oxygen [at $\theta = 0.5$ (*11*)]; S^* and $S^0_{(O)}$ are partial molar quantities involving the entropy change of a catalyst itself during the formation of the activated complex and oxygen adsorption on its surface, respectively. So, $S^* = \Delta S_2^* + S^0_{NH_3} + S^0_{(O)}$. At the temperatures of the catalytic oxidation of ammonia $S^0_{NH_3} =$ 49–53 e.u. (*13*) (at $P = 1$ atm); the $S^0_{(O)}$ mean value for various transition metal oxides calculated after (*14*) is 6 e.u. Then the S^* value found using experimental data will be 27 ± 3 e.u. This quantity is too high for adsorbed species possessing only vibra-

tional degrees of freedom with high frequencies (*15*). Chemical bonds in the activated complex, for example N–H bonds, are probably weakened and characterized by low vibrational frequencies; rotational motion can also be assumed in the transition state.

Comparison of Rate Equations for Formation of Different Products with Experimental Data

The factors preceding r in Eqs. (4) and (5) are selectivites in nitrogen and nitrous oxide:

$$S_{N_2} = \frac{\mu}{\mu + \theta}, \qquad (9)$$

$$S_{N_2O} = \frac{\theta}{\mu + \theta}. \qquad (10)$$

These expressions show that the selectivity of a catalyst at constant temperature must be determined by the oxygen coverage θ which in its turn depends on the mixture composition (P_{O_2}/P_{NH_3} ratio). Equation (7) suggests that θ will increase with increasing P_{O_2}/P_{NH_3}: $\theta \to 0$ at $P_{O_2}/P_{NH_3} \to 0$ and $\theta \to 1$ at $P_{O_2}/P_{NH_3} \to \infty$.

The expected trend will be a progressive decreasing of selectivity in mild oxidation (N_2 formation) and an increasing of selectivity in deep oxidation (N_2O formation) with the increase of P_{O_2}/P_{NH_3} (or θ) since $\partial S_{N_2}/\partial\theta = -\mu/(\mu+\theta)^2 < 0$, $\partial S_{N_2O}/\partial\theta = -\partial S_{N_2}/\partial\theta > 0$. Equations (9) and (10) predict that at $\theta \to 0$ the value of S_{N_2} approaches unity while $S_{N_2O} \to 0$. At $\theta \to 1$ the selectivities approach constant values of $\mu/(\mu+1)$ and $1/(\mu+1)$, respectively.

Using the selectivity value for a single test one can calculate [employing Eq. (9) or (10) together with Eq. (7)] the value of μ, and then one can compute the dependence of selectivity on θ or P_{O_2}/P_{NH_3} expected on the basis of the above equations

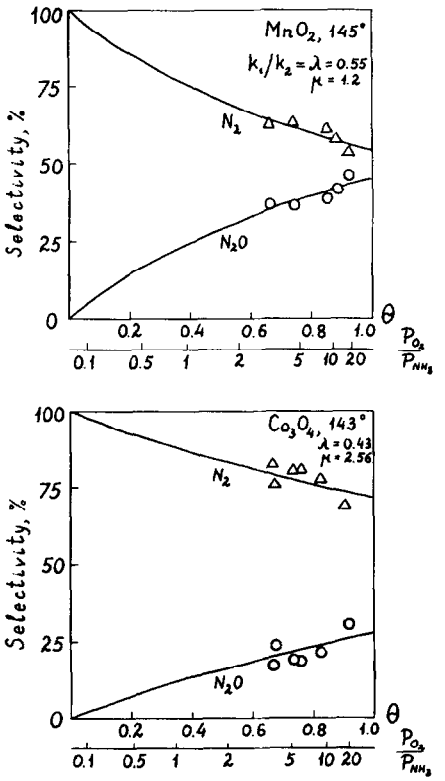

FIG. 6. Dependence of selectivities on θ and P_{O_2}/P_{NH_3} for MnO_2, Co_3O_4.

over a wide range of the reaction mixture compositions. The results of the calculation for various catalysts are presented in Figs. 6 and 7 by smooth curves. The satisfactory agreement with experimental data (points on Figs. 6 and 7) is evidence for the validity of Eqs. (9) and (10). Definite deviations from the theoretical curves are not systematic and should be attributed mainly to the approximations in the theoretical model.

Kinetic results allow us to discriminate (within the scheme proposed) between the above accepted assumption about the two-site adsorption of HNO and that of the one-site adsorption. In the latter case the third stage of scheme (IV) will be:

$$(NH) + (O) \rightleftarrows (HNO) + (\ \ ),$$

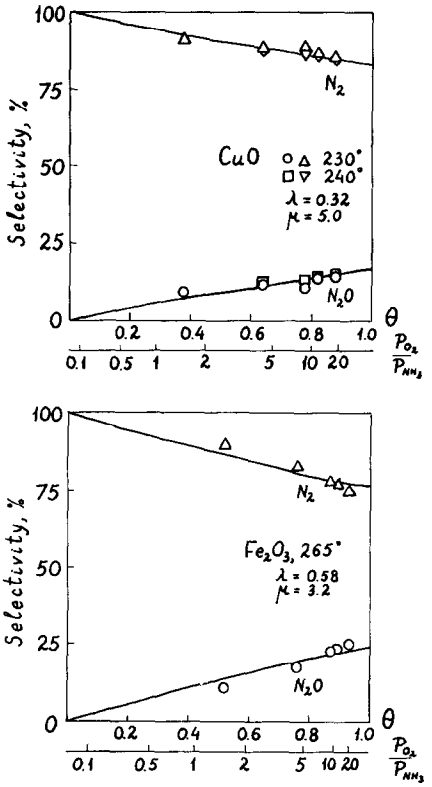

FIG. 7. Dependence of selectivities on θ and P_{O_2}/P_{NH_3} for CuO, Fe_2O_3.

which leads to equations

$$S_{N_2} = \frac{(1-\theta)}{\theta + \mu(1-\theta)}, \qquad S_{N_2O} = \frac{\theta}{\theta + \mu(1-\theta)}. \tag{11}$$

Figure 8 shows that these expressions do not describe the experimental data. That is why the first assumption should be preferred.

According to (IV) the first stage is irreversible. Let us examine an alternative situation when the oxygen desorption rate r_{-1} is rather fast so that in the first stage the adsorption equilibria are attained. Hence θ is determined by the adsorption isotherm

$$\theta = \frac{(bP_{O_2})^{1/2}}{1 + (bP_{O_2})^{1/2}}, \tag{12}$$

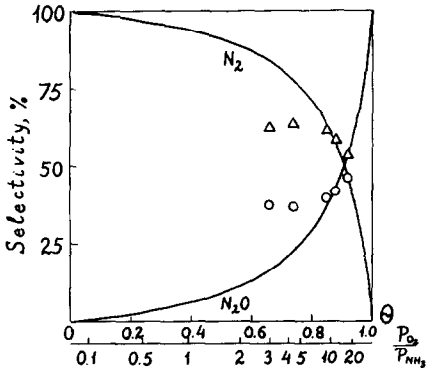

FIG. 8. Dependence of selectivities on θ and P_{O_2}/P_{NH_3} for MnO_2. Smooth curves have been calculated using Eq. (11).

where b is the oxygen adsorption coefficient. The overall reaction rate will be equal to the rate of the second stage which is the limiting one, i.e.,

$$r = \tfrac{1}{2}k_2 P_{NH_3}\theta = \tfrac{1}{2}k_2(b)^{1/2} \cdot \frac{(P_{O_2})^{1/2} \cdot P_{NH_3}}{1 + (bP_{O_2})^{1/2}}.$$

If this is the case, deviations from the linear plots (P_{O_2}/r)–(P_{O_2}/P_{NH_3}) should be observed, because now we have

$$\frac{P_{O_2}}{r} = \frac{2(P_{O_2})^{1/2}}{k_2(b)^{1/2} \cdot P_{NH_3}} + \frac{2}{k_2} \cdot \frac{P_{O_2}}{P_{NH_3}}$$

instead of Eq. (8).

Equations (9) and (10) for selectivities keep their validity but the θ-values are now determined by Eq. (12) instead of Eq. (7):

$$S_{N_2} = \frac{\mu}{\mu + \{(bP_{O_2})^{1/2}/[1 + (bP_{O_2})^{1/2}]\}}, \qquad S_{N_2O} = \frac{(bP_{O_2})^{1/2}/[1 + (bP_{O_2})^{1/2}]}{\mu + \{(bP_{O_2})^{1/2}/[1 + (bP_{O_2})^{1/2}]\}}. \tag{13}$$

It means that at a given temperature and P_{O_2} the selectivity should be a constant quantity independent of P_{NH_3}. According to our data, at P_{O_2} = const the selectivities change with P_{NH_3}, which contradicts Eq. (11). According to Eq. (9) [together with

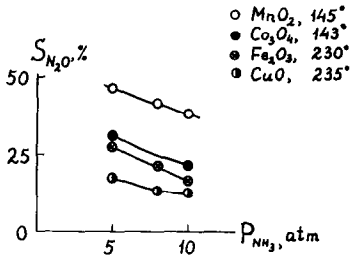

FIG. 9. Relation between selectivity in N_2O and P_{NH_3} at $P_{O_2} = 0.8$ atm.

Eq. (7)] at constant P_{O_2}

$$S_{N_2O} = \frac{1}{a + k' P_{NH_3}}, \qquad (14)$$

where $a = \mu + 1$ and $k' = \mu\bar{\nu}k_2/k_1P_{O_2}$ (a and k' are constants). Fig. 9 demonstrates that the selectivity in nitrous oxide falls with increasing P_{NH_3} which is in accordance with Eq. (14).

Thus, the rate equations deduced on the basis of scheme (IV) agree with the experimental data. This proves the scheme to reflect the essential features of the reaction mechanism under the investigated conditions.

Detailed Reaction Mechanism

Scheme (IV) has been detailed to the extent which was necessary for deducing rate equations: it presents only a composition of intermediates but does not reveal their charges, configurations, etc. Let us now consider the reaction mechanism in more detail.

The first stage results in the formation of surface atomic oxygen which participates in subsequent steps of the process. During the O_2 adsorption on surfaces of semiconducting oxides oxygen usually acts as an electron acceptor and is charged negatively (*16*). Therefore (O) denotes adsorbed atomic anions of oxygen.

The participation of the (O) species in the process as well as the governing role of their surface concentration θ in the reaction kinetics have been independently proved by the similarity in regularities of the catalytic oxidation of ammonia and the surface reduction of oxides with ammonia (in the absence of O_2 in the gas phase). The preliminary treatment of the samples before reduction was carried out under conditions where oxide surfaces contained only atomic oxygen. The following results were obtained.

1. The same products are formed during catalysis and reduction.

2. Rates of the overall conversion of ammonia during reduction fall with the increasing reduction duration τ'. For illustration, Fig. 10a–c, present the respective data for V_2O_5 and CuO. This fact is in agreement with Eq. (3) since θ progressively falls with increasing τ'.

If reduction is made after the treatment of a catalyst with oxygen when an initial surface is in an oxidized state and oxygen coverage is maximal, the starting reduction rate is higher than the steady rate of catalysis (see Fig. 10a). At a definite τ' the reduction rate becomes equal to the rate of catalysis. It corresponds to the A crossing-point of the curves; in this point the values of θ for catalysis and reduction are the same. The evaluation of θ for catalysis [using Eq. (7)] leads to $\theta = 0.96$ indicating

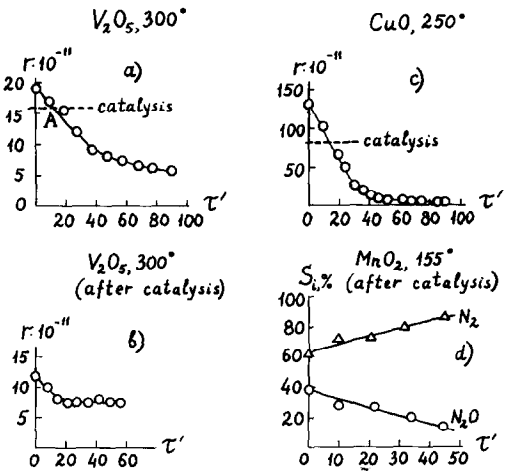

FIG. 10. Rates and selectivities for surface reduction against reduction time [τ' (min)].

the catalytic oxidation to occur on a partially reduced surface.

If reduction is made immediately after catalysis when the initial surface is in a partially reduced state, the observed dependence of reduction rates on τ' (Fig. 10b) is the continuation of the Fig. 10a curve after Point *A*. The initial rate in the former case (Fig. 10b) is somewhat lower than that at Point *A* because of the possible removal of oxygen from V_2O_5 during the substituting of the catalytic mixture ($NH_3 + O_2$) for the reductive one (NH_3 + He).

3. In accordance with Eqs. (9) and (10) the selectivity in N_2 increases and the selectivity in N_2O decreases with increasing τ', i.e., with decreasing θ (Fig. 10d).

The similarity in the regularities of the catalytic oxidation of ammonia and the surface reduction of oxides with ammonia suggests that during the interaction of NH_3 with a surface [the second stage of scheme (IV)] an electron transfer from ammonia to catalyst takes place, so NH_3 acts as an electron donor. This agrees with the results of studies (*3*) where catalytic properties of oxides in ammonia oxidation were related to their semiconducting properties.

It is natural to believe that the hydrogen abstraction from ammonia occurring simultaneously with the electron transfer from NH_3 to a catalyst involves several stages; the formation of final products from NH_3 and O_2 in one stage would require the meeting of many particles which is hardly probable. For proving the participation of (NH) and (HNO) (or maybe other species) in the process the use of some physical methods of investigation is necessary. In this connection it is noteworthy that the most probable products of the interaction of NH_3 with surface oxygen of Fe_2O_3 at lower temperatures according to infrared data (*17*) are nitroxyl-type species.

By means of the ESR technique (*18*) it has been shown that during ammonia adsorption on partially reduced vanadium pentoxide deposited on silica gel the NH_3 molecule enters the first ligand sphere of V^{4+} ions with tetrahedral coordination. As a result of this, a rearrangement of the coordination sphere occurs and a shortened vanadium–oxygen bond appears, this fact being indicative for the formation of vanadyl ions. The above formation of the loose coordination compound can be an initial step in the activation of NH_3 during the catalytic process; this renders possible the subsequent electron transfer. Such a situation appears to be probable because the transition metal cations are inclined to form complexes with ammonia possessing an unshared electron pair.

In further stages of the catalytic process (NH) and (HNO) species like ammonia also act as electron donors. During the conversion of these particles into the reaction products (N_2, N_2O, H_2O) electrons are liberated. Therefore vacant surface sites arising from the fourth and the fifth stages of scheme (IV) are associated with the reduced form of the catalyst cation Me^{n+}_{red} which is able to give electrons. During the adsorption of electron-accepting molecules of oxygen on these sites electrons are transferred to O_2 which results in the formation of atomic negative ions (O), bound with the oxidized form of the cation Me^{m+}_{ox}. It follows from this that the (O) surface concentration, θ, will be proportional to $[Me^{m+}_{ox}]$ while the concentration of vacant sites, $1 - \theta$, will be proportional to $[Me^{n+}_{red}]$ and the ratio of the oxidized to the reduced form, $\gamma = [Me^{m+}_{ox}]/[Me^{n+}_{red}]$, under steady conditions of catalysis will be proportional to $\theta/(1 - \theta)$. According to Eq. (7) this means that γ will be proportional to P_{O_2}/P_{NH_3}.

The same factor determines selectivity of a catalyst at a given temperature. The higher P_{O_2}/P_{NH_3} ratios correspond to the higher surface coverages with oxygen θ. *Because the activated complex of the stage leading to N_2O involves more atoms of oxygen than that of the stage leading to*

N_2 [compare stages (4) and (5)] *the elevated* P_{O_2}/P_{NH_3} *values are favorable for selectivity in the formation of more oxidized product* (N_2O).

Rate Equations for the Process Involving Formation of N_2, N_2O *and NO*

So far there are no experimental data concerning the situation when all three processes (I)–(III) occur simultaneously in the kinetic regime. The reason is the fact that at high temperatures required for process (III) a strong diffusional retardation appears (*1,2*). Nevertheless it is useful to predict some trends expected for the above-mentioned situation.

Let us show that the reaction scheme (IV) can be readily extended with a third parallel reaction (III). In this case ammonia oxidation follows three independent routes associated with Eqs. (I)–(III). Route $N^{(III)}$ is deduced from scheme (IV) if the latter is extended by the stage of the formation of NO. Let us assume the reaction

$$6.\ 2\,(HNO) + (O) \rightarrow 2\,NO + H_2O + 5\,(\ )$$

to be such a stage. Then the reaction mechanism will be

	Stoichiometric nos.[a]		
	$N^{(I)}$	$N^{(II)}$	$N^{(III)}$
1. $O_2 + (\ ) \rightarrow (O_2) \xrightarrow{(\ )}_{fast} 2(\ )$	1.5	2	2.5
2. $NH_3 + (O) \rightarrow (NH) + H_2O$	2	2	2
3. $(NH) + (O) \rightleftarrows (HNO)$	1	2	2
4. $(NH) + (HNO) \rightarrow N_2 + H_2O + 3(\ )$	1	0	0
5. $(HNO) + (HNO) \rightarrow N_2O + H_2O + 4(\ )$	0	1	0
6. $2(HNO) + (O) \rightarrow 2NO + H_2O + 5(\ )$	0	0	1

(V)

[a] $N^{(I)}$: $2NH_3 + 1.5O_2 = N_2 + 3H_2O$; $N^{(II)}$: $2NH_3 + 2O_2 = N_2O + 3H_2O$; $N^{(III)}$: $2NH_3 + 2.5O_2 = 2NO + 3H_2O$.

Equation (3) for the overall process rate keeps its validity. The equations for selectivities will be

$$S_{N_2} = \frac{\mu}{\mu + \theta + \mu'\theta^2}, \tag{15}$$

$$S_{N_2O} = 1 - \frac{\mu}{\mu + \theta + \mu'\theta^2} - \frac{\theta}{(1/\mu') + \theta + (\mu/\mu'\theta)}, \tag{16}$$

$$S_{NO} = \frac{\theta}{(1/\mu') + \theta + (\mu/\mu'\theta)}, \tag{17}$$

where μ is again determined by Eq. (6) while $\mu' = k_6/k_5$ (k_6 is the rate constant for the sixth stage).

The heat effect for the sixth stage is significantly less than that for the fifth one. Actually, the difference between the heats of these stages is $q_6 - q_5 = 2\,q_{NO} - q_{(O)} - q_{N_2O}$ where q_i are the formation heats for the participants of the reaction; $2\,q_{NO} - q_{N_2O} = -23.7$ kcal/mole (*13*) and because of the exothermicity of oxygen adsorption the difference $q_6 - q_5$ is essentially negative. The Brønsted–Polanyi–Temkin relation suggests that higher activation energies are associated with lower heats of stages. If the last two stages of scheme (V) are considered to be similar ones, the activation energy for the sixth stage should be higher than that for the fifth one so that the μ'-value should increase with temperature.

At lower temperatures the μ'-value is close to zero; Eq. (17) shows that under these conditions $S_{NO} \approx 0$ and Eqs. (15) and

(16) coincide with Eqs. (9) and (10). At higher temperatures the μ'-value should be high and S_{NO} should be significant. This conclusion agrees qualitatively with the fact that the formation of NO on a catalyst usually starts at elevated temperatures (*1–4*).

Equations (15)–(17) predict the following. With the mixtures enriched by ammonia (at $P_{O_2}/P_{NH_3} \to 0$ and $\theta \to 0$) S_{N_2} approaches 1 while $S_{NO} \to 0$. On increasing the O_2 excess in the reaction mixture (i.e., on increasing θ) S_{N_2} falls approaching the constant quantity $\mu/(\mu + 1 + \mu')$ (at $\theta \to 1$) while S_{NO} approaches $\mu'/(\mu + 1 + \mu')$. The relation between S_{N_2O} and θ in the general case involves a maximum. For illustration of all these conclusions, Fig. 11 presents the results of a model calculation of the selectivity dependence on θ and P_{O_2}/P_{NH_3} at $\mu' = 100$ (smooth curves) and at $\mu' = 10$ (broken lines); for both cases $k_1/k_2 = \bar{\nu} = \mu = 1$. One can see that the higher values of μ' are associated with the higher selectivities in NO and the lower selectivities in N_2 and N_2O. It should be noted that the above calculation presupposes the reaction to be occurring under a kinetic regime according to the parallel scheme, which is true at not too high conversions of ammonia. Under industrial conditions the NH_3 oxidation proceeds under a diffusional regime at practically complete conversions of ammonia when the consecutive scheme should also be taken into consideration; therefore the dependences observed under these conditions are more complicated (*2*).

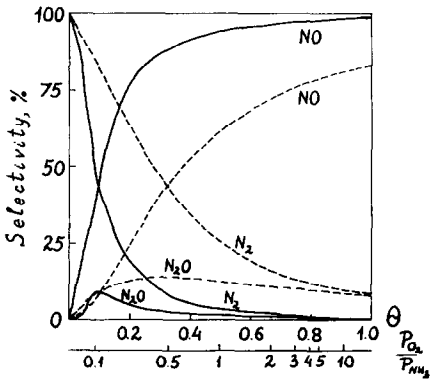

FIG. 11. Dependence of selectivities in N_2, N_2O and NO on θ and P_{O_2}/P_{NH_3} (theoretical curves).

The proposed schemes of the reaction mechanism can serve as the basis for the prediction of the catalytic activity of substances in ammonia oxidation (*19*). This problem is examined in Part II (*20*).

REFERENCES

1. Dixon, J. K., and Longfield, J. E., *in* "Catalysis" (P. H. Emmett, Ed.), Vol. 7, p. 281. Reinhold, New York, 1960.
2. Atroshchenko, V. I., and Kargin, S. I., "Tekhnologia Azotnoi Kisloty." Chimia, Moscow, 1970; Morekhin, M. G., Yakovlev, V. S., and Sidorovitch, A. G., *Ukrain. Khim. Zh.* **28,** 645 (1962).
3. Giordano, N., Cavaterra, E., and Zema, D., *Chem. Ind. (Milan)* **45,** 15 (1963); *J. Catal.* **5,** 325 (1966).
4. Germain, J. E., and Perez, R., *Bull. Soc. Chim. Fr.* **5,** 2042 (1972).
5. Stephens, E. R., and Pease, R. N., *J. Amer. Chem. Soc.* **72,** 1187 (1933).
6. Saito, Y., Yoneda, Y., and Makishima, S., *Actes Congr. Int. Catal., 2nd, 1960* **1,** 1937 (1961).
7. Winter, E. R. S., *J. Catal.* **19,** 32 (1970).
8. Mashchenko, A. I., Kazanskii, V. B., Parijskii, G. B., and Sharapov, V. M., and Kazanskii, V. B., *Kinet. Katal.* **10,** 356 (1969); Van Hooff, G. H. C., Van Helden, J. F., *J. Catal.* **8,** 199 (1967).
9. Horiuti, J., *J. Res. Inst. Catal. Hokkaido Univ.* **5,** 1 (1957).
10. Temkin, M. I., *Dokl. Akad. Nauk SSSR* **152,** 156 (1963).
11. Temkin, M. I., *Zh. Fiz. Khim.* **11,** 169 (1938); **14,** 1054 (1940).
12. Golodets, G. I., and Roiter, V. A., *Kinet. Katal.* **4,** 177 (1963).
13. Wicks, C. E., and Block, F. E., "Thermodynamic Properties of 65 Elements–Their Oxides, Halides, Carbides and Nitrides." US Dept. of Interior 1965 (Russ. Transl.).
14. Kul'kova, N. V., and Temkin, M. I., *Zh. Fiz. Khim.* **31,** 2017 (1957).
15. Kemball, C., *in* "Advances in Catalysis" (W. G. Frankenburg, V. I. Komarewsky and E. K. Rideal, Eds.), Vol. 2, p. 233. Academic Press, New York, 1950.

16. Margolis, L. Y., "Heterogennoje Kataliticheskoje Okislenie Uglevodorodov." Chimia, Leningrad, 1967.
17. Griffiths, D. W. L., Hallam, H. E., and Thomas, W. J., *J. Catal.* **17,** 18 (1970).
18. Vorotintsev, V. M., Shvets, V. A., and Kazanskii, V. B., *Kinet. Katal.* **12,** 678 (1971)
19. Il'chenko, N. I., and Golodets, G. I., *Theor. Exp. Khim.* **9,** 36 (1973); *Katal. Katal.* **11,** 3 (1974).
20. Il'chenko, N. I., and Golodets, G. I., *J. Catal.* **39,** 73 (1975).